An Adaptive Control Scheme for Mechanical Manipulators—Compensation of Nonlinearity and Decoupling Control

Roberto Horowitz
Graduate Student.[1]

Masayoshi Tomizuka
Associate Professor.
Mem. ASME

Department of Mechanical Engineering,
University of California, Berkeley, CA 94720

This paper presents a new adaptive control scheme for mechanical manipulators. Making use of the fundamental properties of the manipulator equations, an adaptive algorithm is developed for compensating a nonlinear term in the dynamic equations and for decoupling the dynamic interaction among the joints. A computer simulation study is conducted to evaluate the performance of a manipulator control system composed of the manipulator, adaptive nonlinear compensator/decoupling controller and state feedback controller with integral action. Simulation results show that the manipulator control system with adaptive controller is insensitive to variations of manipulator configurations and payload.

I Introduction

A mechanical manipulator can be defined as a multidegree of freedom open loop chain of mechanical linkages and joints. These mechanisms driven by actuators are capable of moving an object in space from initial to final locations or along prescribed trajectories.

The dynamic equations of a mechanical manipulator are highly nonlinear and complex. The inertia characteristics of the manipulator depend on the payload also. To overcome these difficulties, a number of techniques for dynamic control of mechanical manipulators have been proposed. In the computed torque drive method [1, 2, 3], the torques required to move the manipulator along a prescribed trajectory are numerically computed using the dynamic equations. A disadvantage of this method is that a considerable amount of computational effort is required to solve the equations, making its use difficult in real time control. The resulting control, if used without closed loop feedback, is subject to problems inherent in open loop control. To increase the computational speed, table look-up control methods have been proposed where data pertaining to manipulator characteristics are stored and are retrieved as needed [4]. Combinations of the torque drive methods and the table look-up methods are also possible [5]. The dynamic equations are often linearized about nominal trajectories, and linear feedback and/or optimal control laws are obtained analytically [6, 7]. The use of nonlinear feedback compensation has been proposed for making the equations of motion linear in simple locomotion systems [8]. The nonlinear compensation is either computed in real time or retrieved from memory storage.

In general, a detailed description of the model and information on load characteristics are required in the methods described above. To relax these requirements, a considerable amount of effort has been devoted to the development of new techniques. Recently proposed techniques include the use of the theory of the variable structure systems [9, 10] and a model reference adaptive control approach [11].

This paper presents a new adaptive scheme, different from the one in [11], for dynamic control of mechanical manipulators. After discussing the kinematics and dynamics of mechanical manipulators, the fundamental properties of the manipulator equations are stated in Section II. Making use of the fundamental properties, a simple adaptive algorithm for compensation of a nonlinear term in the manipulator equations and decoupling control is derived in Section III. Section IV presents the simulation results of a manipulator control system composed of the manipulator, adaptive nonlinear compensator/decoupling controller and state feedback controller with an integral action. A discussion of future research items is also given.

II Mathematical Model of Mechanical Manipulators

2.1 Kinematics. In order to define the location (position and orientation) of a rigid body in space, it is necessary to specify six independent coordinates. Although an adaptive control scheme in the next section is for positioning of a three degree of freedom manipulator, the mathematical modelling is discussed for a general mechanical manipulator composed of linkages connected by cylindrical, revolute or prismatic joints. Most existing manipulators are built with only revolute or prismatic joints. A cylindrical joint permits the two connected links to slide and rotate along its axis. A revolute joint can be treated as a cylindrical joint which does not permit sliding while a prismatic joint can be treated as a cylindical joint which does not permit rotation along its axis.

A six degree of freedom manipulator is sketched in Fig. 1. Symbols in the figure are defined as follows:

[1] Presently Assistant Professor.

Contributed by the Dynamic Systems and Control Division of THE AMERICAN SOCIETY OF MECHANICAL ENGINEERS and presented at the Winter Annual Meeting, Chicago, Ill., November 16-21, 1980. Manuscript received at ASME Headquarters, February 6, 1986. Paper No. 80-WA/DSC-6.

Copyright © 1986 by ASME
Downloaded From: http://dynamicsystems.asmedigitalcollection.asme.org/ on 04/09/2015 Terms of Use: http://asme.org/terms

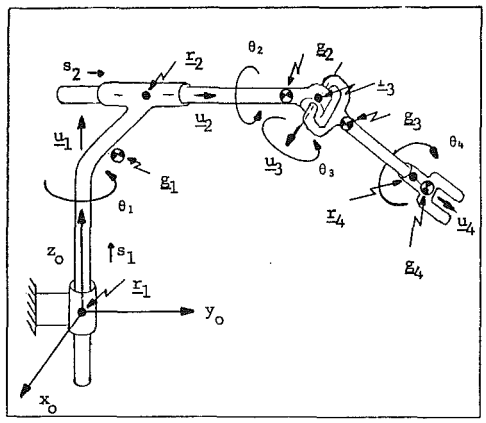

Fig. 1 Mechanical manipulator

$\mathbf{r}_i$ = 3 dimensional position vector of joint between link i-1 and link i,

$\mathbf{g}_i$ = 3 dimensional vector of center of mass of link i,

$\mathbf{u}_i$ = 3 dimensional unit vector of rotation and/or sliding axis of joint i,

θ_i = rotation angle along axis $\mathbf{u}_i$,

and

s_i = sliding displacement along axis $\mathbf{u}_i$.

All vectors are specified with respect to the fixed or reference coordinate system (x_0, y_0, z_0).

The kinematic analysis of mechanical manipulators is in general a complex problem by itself. Two different problems are: 1. given the angular rotations and slidings of the joints, determine the location of the end effector, and 2. given the desired location of the end effector, determine the required angular rotations and slidings of the joints. The second problem is much more difficult to solve than the first. In general, unless some additional constraints are imposed on the configuration of the manipulator, it leads to the solution of six nonlinear algebraic equations or the finding of the roots of a polynomial depending on the method of analysis used [12–14].

2.2 Dynamics. For a $2n$ degree of freedom manipulator composed of n rigid links connected by n ideal cylindrical joints, defining the generalized coordinates as

$$\xi^T = [\xi_\theta^T \xi_s^T] = [\theta_1 \theta_2 \ldots \theta_n s_1 s_2 \ldots s_n] \tag{1}$$

and using equation (3), the dynamic equations of the manipulator are obtained in the form,

$$\mathbf{M}(\xi)\cdot\ddot{\xi} + \mathbf{v}(\xi,\dot{\xi}) = \mathbf{q} \tag{2}$$

where $\mathbf{M}$ (ξ) is the $2n \times 2n$ generalized inertia matrix, $\mathbf{q}$ is the $2n$ dimensional generalized force vector (which includes torques and sliding forces at joints, potential forces, friction forces etc.), and $\mathbf{v}(\xi, \dot{\xi})$ is a $2n$ dimensional vector given by

$$\mathbf{v} = \begin{bmatrix} v_1 \\ v_2 \\ \cdot \\ \cdot \\ \cdot \\ v_{2n} \end{bmatrix} = \begin{bmatrix} \dot{\xi}^T \mathbf{N}^1(\xi)\dot{\xi} \\ \dot{\xi}^T \mathbf{N}^2(\xi)\dot{\xi} \\ \cdot \\ \cdot \\ \cdot \\ \dot{\xi}^T \mathbf{N}^{2n}(\xi)\dot{\xi} \end{bmatrix} \tag{3}$$

For the detailed structure of $\mathbf{M}$ and $\mathbf{N}^k$'s, see Appendix I. If the ith joint is revolute (or prismatic) instead of cylindrical, s_i (or θ_i) together with corresponding equation must be deleted from (2) and (3). Assuming that such deletions have been done for all joints, $\mathbf{M}$ and $\mathbf{N}^k$'s in the manipulator equation satisfy the following lemma.

Lemma: For a mechanical manipulator composed of links connected by ideal cylindrical, revolute or prismatic joints,

A. The generalized inertia matrix is symmetric and positive definite: i.e.,

$$m_{ij} = m_{ji} \text{ and } \mathbf{M} > 0, (i,j = 1,2, \ldots, 2n) \tag{4}$$

B. The matrices, $\mathbf{N}^k$'s, satisfy

$$n_{ij}^k = n_{ji}^k, n_{ik}^k = 0 \text{ and } n_{kj}^i = -n_{kk}^i, (i,j,k = 1,2, \ldots, 2n) \tag{5}$$

where m_{ij} and n_{ij}^k are the i-j element of $\mathbf{M}$ and $\mathbf{N}_{ij}^k$, respectively.

The proof of this lemma is given in Appendix II. Property A will be used in the stability proof of the MRAS schemes in Section III. Properties A and B are also useful in simplifying the adaptation algorithm.

2.3 Three Degree of Freedom Mechanical Manipulator. In the remaining portion of this paper, a three degree of freedom manipulator with three revolute joints will be considered. A schematic drawing of the manipulator is shown in Fig. 2. This manipulator is essentially the same as the one used in [11]. The manipulator is balanced and two revolute axes, $\mathbf{u}_2$ and $\mathbf{u}_3$, remain parallel to each other. To simplify the dynamic analysis and simulation, the following assumptions were made: 1. the gravity can be neglected, 2. the inertia moments of link 1 and of the payload are negligible, and 3. the position mass and moment of inertia of link 1, and the moment of inertia of the payload are negligible. Under these assumptions, equation (2) yields the following dynamic equations.

$$\begin{bmatrix} m_{11} & m_{12} & m_{13} \\ m_{12} & m_{22} & m_{23} \\ m_{13} & m_{23} & m_{33} \end{bmatrix} \begin{bmatrix} \dot{x}_{v1} \\ \dot{x}_{v2} \\ \dot{x}_{v3} \end{bmatrix} + \begin{bmatrix} v_1(\mathbf{x}_p,\mathbf{x}_v) \\ v_2(\mathbf{x}_p,\mathbf{x}_v) \\ v_3(\mathbf{x}_p,\mathbf{x}_v) \end{bmatrix} = \begin{bmatrix} q_1 \\ q_2 \\ q_3 \end{bmatrix} \tag{6}$$

where $\mathbf{x}_p^T = [x_{p1}\ x_{p2}\ x_{p3}] = [\theta_1\ \theta_2\ \theta_3]$ is the angular rotation vector, $\mathbf{x}_v^T = [x_{v1}\ x_{v2}\ x_{v3}] = [\dot{\theta}_1 \dot{\theta}_2\ \dot{\theta}_3]$ is the angular velocity vector, $\mathbf{q}^T = [q_1\ q_2\ q_3]$ and $\mathbf{v}(\mathbf{x}_p, \mathbf{x}_v)^T = [v_1(\mathbf{x}_p, \mathbf{x}_v)\ v_2(\mathbf{x}_p, \mathbf{x}_v) v_3(\mathbf{x}_p, \mathbf{x}_v)]$

$$\begin{aligned} v_1(\mathbf{x}_p,\mathbf{x}_v) &= \mathbf{x}_v^T \begin{bmatrix} 0 & n_{12}^1 & n_{13}^1 \\ n_{12}^1 & n_{22}^1 & n_{33}^1 \\ n_{13}^1 & n_{33}^1 & n_{33}^1 \end{bmatrix} \mathbf{x}_v \\ v_2(\mathbf{x}_p,\mathbf{x}_v) &= \mathbf{x}_v^T \begin{bmatrix} -n_{12}^1 & 0 & 0 \\ 0 & 0 & n_{33}^2 \\ 0 & n_{33}^2 & n_{33}^2 \end{bmatrix} \mathbf{x}_v \\ v_3(\mathbf{x}_p,\mathbf{x}_v) &= \mathbf{x}_v^T \begin{bmatrix} -n_{13}^1 & 0 & 0 \\ 0 & -n_{33}^2 & 0 \\ 0 & 0 & 0 \end{bmatrix} \mathbf{x}_v \end{aligned} \tag{7}$$

(n_{ij}^k's are functions of x_{p2} and x_{p3})

where equations (4) and (5) have been utilized.

Notice that equations (6) and (7) include eleven coefficients, m_{ij}'s and n_{ij}^k's, which are functions of x_{p2} and x_{p3}.

III Nonlinearity Compensation and Decoupling Control for Mechanical Manipulators

In this section, an adaptive control scheme for mechanical manipulators is developed based on the model reference adaptive systems (MRAS) technique [18]. The manipulator described by equations (6) and (7) will be considered. For this type of manipulators, a model reference adaptive control scheme has been proposed by Dubowsky and DesForges [11].

Downloaded From: http://dynamicsystems.asmedigitalcollection.asme.org/ on 04/09/2015 Terms of Use: http://asme.org/terms

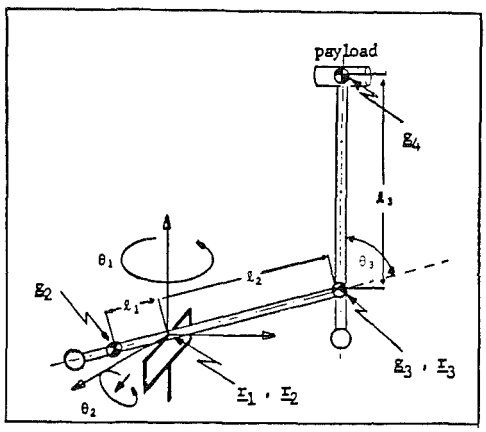

Fig. 2 Three degree of freedom mechanical manipulator

The present adaptive control scheme and the approach to the overall control of manipulators are very different from those in [11]. The overall control system in this paper will have an inner loop MRAS controller and an outer loop proportional, integral and derivative (PID) action controller with fixed gains. The manipulator control system in [11] is entirely based on the model reference adaptive controller. Other differences between the adaptive controller design in [11] and the one presented in this paper are: 1) The adaptation algorithm design in [11] is based on the steepest descent method, followed by a separate stability analysis using linearization. The design method presented in this paper is based on the hyperstability approach [18]. 2) In [11] the coupling among joints and the nonlinear terms in the manipulator equations of motion are neglected in the control design, while in this paper they are explicitly considered.

3.1 Deterministic Nonlinear Compensation and Decoupling Control. To make the role of the adaptive controller clear, we will first consider a control law for the torque input that accomplishes nonlinearity compensation and decoupling assuming that the values of the manipulator parameters are known at all instances. The control law is given by

$$\mathbf{q}(t) = \mathbf{M}(\mathbf{x}_p)u(t) + \mathbf{v}(\mathbf{x}_p, \mathbf{x}_v) \tag{8}$$

where $\mathbf{u}(t)$ is the new external controlling input. From equations (6) and (8), we obtain

$$\dot{\mathbf{x}}_p(t) = \mathbf{x}_v(t) \tag{9}$$
$$\dot{\mathbf{x}}_v(t) = \mathbf{u}(t)$$

Equation (9) represents three decoupled integrators, for which the design of a feedback controller is very simple. It should be noted that the second term in the control law (8) is for cancelling the nonlinear term $\mathbf{v}(\mathbf{x}_p, \mathbf{x}_v)$ in the manipulator equation (6) and $\mathbf{M}(\mathbf{x}_p) > \mathbf{0}$ (see Lemma in Section II) is for decoupling the interaction among the three joints.

3.2 Adaptive Nonlinearity Compensation and Decoupling Control. Implementation of the control law (8) requires the values of $\mathbf{M}(\mathbf{x}_p)$ and $\mathbf{v}(\mathbf{x}_p, \mathbf{x}_v)$ be either computed or stored for all $\mathbf{x}_p$, which is a demanding task for computers in real time control. To avoid this difficulty, we will make the control law adaptive utilizing the MRAS technique: i.e., we will adjust the parameters in the control law so that the $\mathbf{x}_v - \mathbf{u}$(and $\mathbf{x}_p - \mathbf{u}$) relations converge to equation (9).

We will use a reference model described by

$$\dot{\hat{\mathbf{x}}}_p(t) = \hat{\mathbf{x}}_v(t) \tag{10}$$
$$\dot{\hat{\mathbf{x}}}_v(t) = \mathbf{u}(t)$$

where $\hat{\mathbf{x}}_p(t)$ and $\hat{\mathbf{x}}_v(t)$ are the angular position and velocity vectors of the reference model. The torque input vector to the manipulator is

$$\mathbf{q}(t) = \hat{\mathbf{M}}(t)\mathbf{u}(t) + \hat{\mathbf{v}}(t, \mathbf{x}_v) + \mathbf{F}_p[\hat{\mathbf{x}}_p(t) - \mathbf{x}_p(t)] + \mathbf{F}_v[\dot{\hat{\mathbf{x}}}_v(t) - \mathbf{x}_v(t)] \tag{11}$$

$$\hat{\mathbf{v}}(t, \mathbf{x}_v) = [\mathbf{x}_v{}^T\hat{N}^1(t)\mathbf{x}_v, \mathbf{x}_v{}^T\hat{N}^2(t)\mathbf{x}_v, \mathbf{x}_v{}^T\hat{\mathbf{N}}^3(t)\mathbf{x}_v]^T \tag{12}$$

where $\hat{\mathbf{M}}(t)$ and $\hat{\mathbf{N}}(t)$'s are adjusted by the adaptive algorithm given below and the last two terms in equation (11) are for guaranteeing the stability of the adaptive scheme.

The adaptive algorithm for $\hat{\mathbf{M}}(t)$ and nonzero elements of $\hat{\mathbf{N}}(t)$'s is given by

$$\frac{d}{dt}[\hat{m}_{ij}] = k_{mij}[y_i u_j]; \qquad i = 1,2,3 \quad j = 1,2,3 \tag{13}$$

$$\frac{d}{dt}[\hat{n}^k{}_{ij}] = k^k{}_{nij}[y_k x_{vi} x_{vj}]; \quad k = 1,2,3 \quad i = 1,2,3 \quad j = 1,2,3$$

$k_{mij} > 0$, $k^k{}_{nij} > 0$

where

$$\mathbf{y}(t) = \mathbf{C}_p\mathbf{e}(t) + \mathbf{C}_v\dot{\mathbf{e}}(t) \tag{14}$$

and $\mathbf{e}(t)$ and $\dot{\mathbf{e}}(t)$ are the error between the reference model and manipulator angular position vector and angular velocity vector, respectively.

$$\mathbf{e}(t) = \hat{\mathbf{x}}_p(t) - \mathbf{x}_p(t), \dot{\mathbf{e}}(t) = \hat{\mathbf{x}}_v(t) - \mathbf{x}_v(t) \tag{15}$$

$\mathbf{C}_p$ and $\mathbf{C}_v$ are both square and selected by the designer along with $\mathbf{F}_p$ and $\mathbf{F}_v$ in equation (11). A guideline for the selection of matrices $\mathbf{C}_p$, $\mathbf{C}_v$, $\mathbf{F}_p$, and $\mathbf{F}_v$ is given in equations (17) and (18) below.

The main motivation for the adaptive algorithm (13) is to satisfy the Popov inequality (A3-6) which is required to guarantee the stability of the MRAS scheme. The proof (presented in Appendix III) is constructive and the adaptation algorithm (13) naturally comes out.

For a three degree of freedom manipulator, the adaptation algorithm in equation (13) implies that nine $\hat{m}_{ij}(t)$'s and fourteen $\hat{n}^k{}_{ij}(t)$'s are adjustable, giving a total of twenty three parameters which need to be updated by the adaptation algorithm. Fortunally, all of the updating laws in equation (13) are independent of each other, which implies that all twenty three parameters can be updated simultaneously using multiprocessing equipment.

The number of adjustable parameters in the adaptation algorithm can be reduced to eleven (11) by taking into account equations (4) and (5) in the Lemma: i.e. an alternative algorithm for the $\hat{m}_{ij}(t)$'s and $\hat{n}^k{}_{ij}(t)$'s is

$$\frac{d}{dt}[\hat{m}_{ii}] = k_{mii}[y_i u_i]; \; i = 1,2,3$$

$$\frac{d}{dt}[\hat{m}_{ij}] = k_{mij}[y_i u_j + y_j u_i]; \; i = 1,2, j = 2,3, \; i \neq j$$

$$\hat{m}_{ji} = \hat{m}_{ij}$$

$$\frac{d}{dt}[\hat{n}^1{}_{12}(t)] = k^1{}_{n12}[2y_1 x_{v1} x_{v2} - y_2 x_{v1}{}^2]$$

$$\frac{d}{dt}[\hat{n}^1{}_{13}(t)] = k^1{}_{n13}[2y_1 x_{v1} x_{v3} - y_3 x_{v1}{}^2] \tag{13'}$$

$$\frac{d}{dt}[\hat{n}^1{}_{22}(t)] = k^1{}_{n22}[y_1 x_{v2}{}^2]$$

$$\frac{d}{dt}[\hat{n}^1{}_{33}(t)] = k^1{}_{n33}[2y_1 x_{v2} x_{v3} \pm y_1 x_{v3}{}^2]$$

$$\frac{d}{dt}[\hat{n}^2{}_{33}(t)] = k^2{}_{n33}[2y_2 x_{v2} x_{v3} - y_3 x_{v2}{}^2 + y_2 x_{v3}{}^2]$$

Downloaded From: http://dynamicsystems.asmedigitalcollection.asme.org/ on 04/09/2015 Terms of Use: http://asme.org/terms

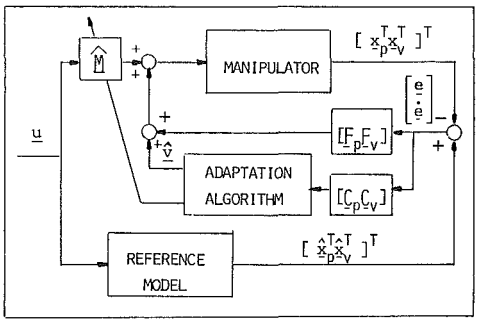

Fig. 3 MRAS nonlinear compensator/decoupling controller for mechanical manipulator

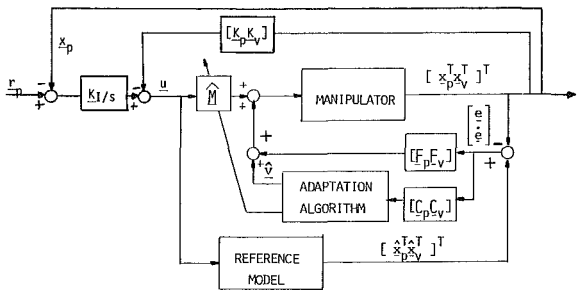

Fig. 4 Mechanical manipulator control system

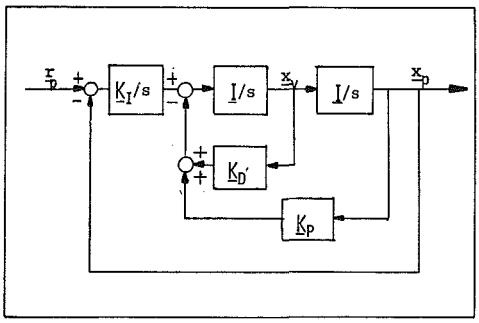

Fig. 5 Ideal system

Figure 3 depicts the MRAS scheme for nonlinearity compensation and decoupling control.

Under the assumption that the parameters, m_{ij}'s and $n^k{}_{ij}$'s, remain constant during the adaptation algorithm, the MRAS can be proven to be assymptotically stable if the transfer function matrix,

$$\mathbf{G}(s) = [\mathbf{C}_v s + \mathbf{C}_p][\mathbf{M}s^2 + \mathbf{F}_v s + \mathbf{F}_p]^{-1} \tag{16}$$

is strictly positive real (see Appendix III for the proof).

A possible set of design parameter matrices, $\mathbf{C}_p$, $\mathbf{C}_v$, $\mathbf{F}_p$, and $\mathbf{F}_v$, to satisfy the last condition is

$$[\mathbf{C}_p\mathbf{C}_v] = [\sigma_p\mathbf{I}\sigma_v\mathbf{I}] \text{ and } [\mathbf{F}_p\mathbf{F}_v] = [\rho_p\mathbf{I}\rho_v\mathbf{I}] \tag{17}$$

where $\mathbf{I}$ is the identity matrix, and the four scalars σ_p, σ_v, ρ_p, and ρ_v are all positive and satisfy

$$\sigma_v > \sigma_p, \sigma_v\rho_v\mathbf{I} - \sigma_p\mathbf{M} > \mathbf{0} \text{ and } [\sigma_v\rho_p + \sigma_p\rho_v]\mathbf{I} - \sigma_p\mathbf{M} > \mathbf{0} \tag{18}$$

This condition can be easily derived from the Kalman-Yakubovitch-Popov Lemma [18] (see [14] for details).

IV Computer Simulation

A computer simulation study was conducted to evaluate the MRAS nonlinear compensator and decoupling controller. The block diagram of the simulated manipulator control system is shown in Fig. 4. As illustrated in the figure, a state vector

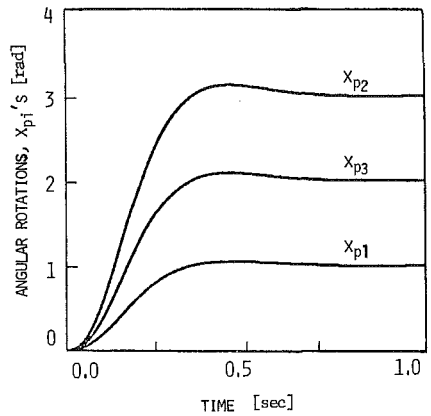

Fig. 6 Step response for ideal system (r_p^T = [1 3 2] rad)

feedback controller with an integral (I) action was added to complete the manipulator control system. The actuators were assumed to have no dynamics and no power limitations. Expecting that the MRAS nonlinear compensator and decoupling controller achieve their objectives, the state vector and I feedback control gain matrices, $\mathbf{K}_p$, $\mathbf{K}_D$, and $\mathbf{K}_I$, were all set to be diagonal matrices with diagonal elements, 500 s^{-2}, 40 s^{-1} and 3000 s^{-3}, respectively. When each $u_i - x_{pi}$ pair dynamics are represented by an ideal double integrator transfer function, these feedback control gains places the closed loop poles of each loop at -24.7, $-7.7+7.93j$, and $-7.7-7.93j$.

The overall control system with the manipulator and MRAS nonlinear compensator/decoupling controller replaced by three double integrators will be called the "ideal system" (see Fig. 5). The step response of the ideal system is shown in Fig. 6 for a step reference input vector, $\mathbf{r}_p^T$ = [1 3 2] rad.

In the simulation of the manipulator control system, the following numerical data were used:

Manipulator Parameters (similar to those in [11])

$\mathbf{I}_1 = \mathbf{0}$ and $m_1 = 0$

$$\mathbf{I}_2 = \begin{bmatrix} 3.348 & 0.05 & 0.5 \\ 0.05 & 0.1 & 0.05 \\ 0.5 & 0.05 & 3.348 \end{bmatrix} [\text{kg}\cdot\text{m}^2],\ m_2 = 23.3 \text{ [kg]}$$

$$\mathbf{I}_3 = \begin{bmatrix} 0.924 & 0.02 & 0.1 \\ 0.02 & 0.1 & 0.02 \\ 0.1 & 0.02 & 0.924 \end{bmatrix} [\text{kg}\cdot\text{m}^2],\ m_3 = 6.71 \text{ [kg]}$$

$l_1 = 0.36$ [m], $l_2 = 0.89$ [m], $l_3 = 0.914$ [m]

where $\mathbf{I}_i$, m_i, and l_i are link i's moment of inertia, mass, and length, respectively, and l_i's are as defined in Fig. 2.

Varying Payload m_p = 5, 10 and 20 [kg]

Adaption Gains

$k_{m11} = 5, k_{m22} = 7, k_{m33} = 5, k_{m23} = 5, k_{m12} = k_{m13} = 0.01$

$k^1_{n12} = 20, k^1_{n13} = 5, k^1_{n22} = k^1_{n33} = k^2_{n33} = 0.01$

Design Parameter Matrices

$[\mathbf{C}_p\mathbf{C}_v] = [\mathbf{I}\ 20\times\mathbf{I}],\ [\mathbf{F}_p\mathbf{F}_v] = [20\times\mathbf{I}\ 20\times\mathbf{I}]$

Initial Condition for $\hat{\mathbf{M}}(t)$ and $\hat{\mathbf{N}}^k(t)$'s

$\hat{m}_{11}(0) = 25, \hat{m}_{22}(0) = 25, \hat{m}_{33}(0) = 5$

$\hat{m}_{12}(0) = 0, \hat{m}_{13}(0) = 0, \hat{m}_{23}(0) = 8$

$\hat{n}^1_{12}(0) = \hat{n}^1_{13}(0) = \hat{n}^1_{22}(0) = \hat{n}^1_{33}(0) = \hat{n}^2_{33}(0) = 0$

Downloaded From: http://dynamicsystems.asmedigitalcollection.asme.org/ on 04/09/2015 Terms of Use: http://asme.org/terms

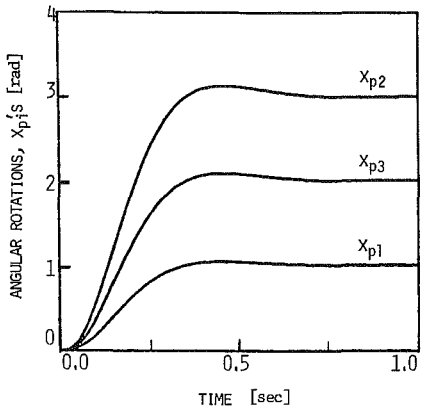

Fig. 7 Step responses of manipulator control system with adaptation (r_p^T = [1 3 2] rad, payload = 10 and 20 Kg)

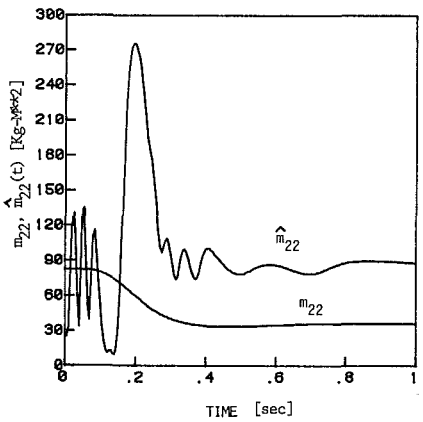

Fig. 8 m_{22} and $m_{22}(t)$ during the step response (r_p^T = [1 3 2] rad, payload = 20 Kg)

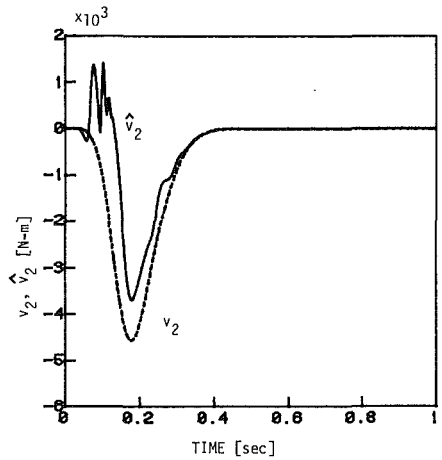

Fig. 9 $v_2(t)$ and $v_2(t)$ during the step response (r_p^T = [1 3 2] rad, payload = 20 Kg)

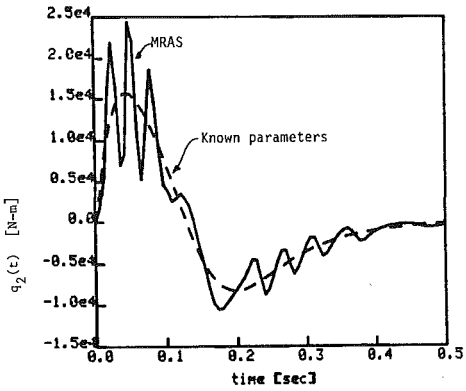

Fig. 10 Torque input to joint 2, $q_2(t)$. (payload = 20 Kg)

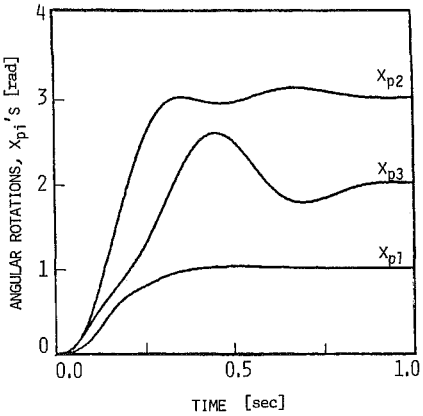

Fig. 11 Step response of manipulator control system without adaptation (r_p^T = [1 3 2] rad, payload = 5 Kg)

The initial value of $\hat{\mathbf{M}}(t)$ is an approximate average of the varying $\mathbf{M}$ matrix of the manipulator when moving a payload of 5 kg from $\mathbf{x}_p^T = [0\ 0\ 0]$ rad to $\mathbf{x}_p^T = [0\ 2\pi\ 2\pi]$rad.

Figure 7 shows the step responses of the manipulator control system in Fig. 4 for a step reference input vector, $\mathbf{r}_p^T$ = [1 3 2] rad when the payload is 10 kg and 20 kg. Two response curves overlayed are indistinguishable, which implies that the system is insensitive to payload variations. Moreover, these responses are essentially the same as the one in Fig. 6 (ideal system response), which implies that the MRAS nonlinear compensator/decoupling controller is achieving its objective successfully. Some of the adjustable parameters are plotted in Figs. 8 and 9. It is obvious in Fig. 8 that the adjustable parameter $\hat{m}_{22}$ does not converge to the true value. It should be noted that the stability of the MRAS only guarantees the output error to converge to zero, and that it does not guarantee nor require the parameter error to converge to zero. The parameter error converges to zero when the input signal is *sufficiently rich in its frequency content*. Noting that all the parameter vary during the transient and that the step reference input contains only one frequency component (DC) asymptotically, the parameter error convergence to zero is not expected in the present MRAS. However, the MRAS certainly achieves its objective vanishing the output error between the reference model and manipulator.

Figure 10 shows the torque input $q_2(t)$, which is necessary to achieve the ideal trajectory shown in Fig. 6, assuming that all the parameters, m_{ij}'s and n_{ij}^k's are precisely known (dashed line). Also shown in the figure is the torque input $q_2(t)$ when the manipulator is under adaptive control. As shown by this figure, the adaptive controller does not impose unrealistic high torque inputs when compared with the torque inputs required for the case where the parameters are precisely known.

To appreciate the improvement gained by the MRAS nonlinear compensator/decoupling controller, the simulation was repeated inactivating the adaptation algorithm: i.e., the decoupling matrix $\hat{\mathbf{M}}$ was kept constant ($\hat{\mathbf{M}}(0)$) and no compensation for the nonlinearity, $\mathbf{v}$, was made. The step responses of the nonadaptive manipulator control system for payloads of 5 kg and 20 kg are shown in Figs. 11-12. The results show that the system performance without adaptation

Downloaded From: http://dynamicsystems.asmedigitalcollection.asme.org/ on 04/09/2015 Terms of Use: http://asme.org/terms

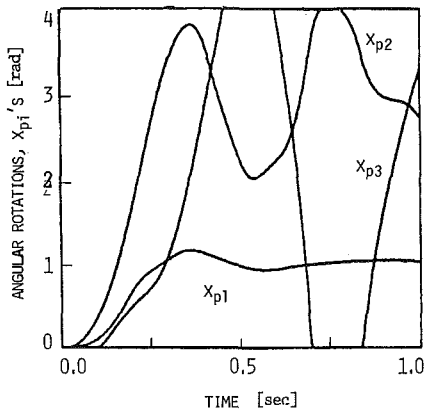

Fig. 12 Step response of manipulator control system without adaptation
(r_p^T = [1 3 2] rad, payload = 20 Kg)

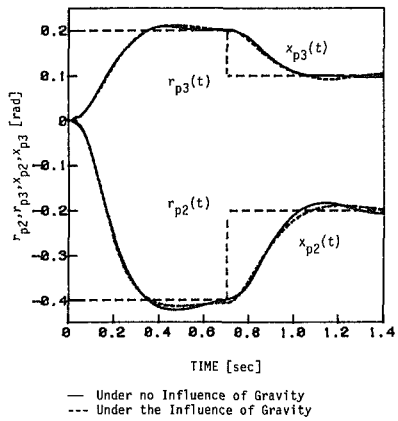

Fig. 13 Effect of gravity upon the response of manipulator control system with adaptation
(payload = 20 Kg)

is highly sensitive to variations of payload and manipulator configuration.

The next set of simulations was conducted to evaluate the effect of gravity which was neglected in the design of the adaptive controller. In these simulations, the adaptive algorithm (13) was used and the payload was $m_p = 20$ kg. Initial conditions for $\hat{\mathbf{M}}(t)$ and $\hat{N}^k(t)$ were the same as before except for $\hat{m}_{23}(t)$ and $\hat{m}_{32}(t)$ which were both equal to zero. The adaptation gains were

$$k_{m11} = k_{m22} = k_{m33} = k_{m23} = k_{m32} = 5,$$
$$k_{m12} = k_{m21} = k_{m13} = k_{m31} = 0 \tag{19}$$
$$k^1_{n12} = k^1_{n13} = 5, k^1_{n22} = k^1_{n33} = k^2_{n33} = 0$$

The gains that were set to zero correspond to the parameters whose actual values are negligible. The reference input $\mathbf{r}_p(t)$ is shown by the dashed line in Fig. 13. The solid line in Fig. 13 represents the response of the manipulator under no influence of gravitational forces, and the dotted line represents the response under influence of gravitational forces. The results show that the effect of the gravity is small, which is attributed to the combined effect of the I-action in the outer feedback loop and the time varying decoupling matrix $\hat{\mathbf{M}}(t)$.

During the course of the simulation study, it was found that the adaptive control scheme can be drastically simplified by neglecting some of the adjustable parameters. The effect of the nonlinear term $\mathbf{v}(\mathbf{x}_p, \mathbf{x}_v)$ was secondary in most of the simulated conditions, and deleting $\hat{\mathbf{v}}(t, \mathbf{x}_v)$ did not cause any essential change in the response. Adjusting only the diagonal elements of $\hat{\mathbf{M}}(t)$ and leaving others zero yielded satisfactory

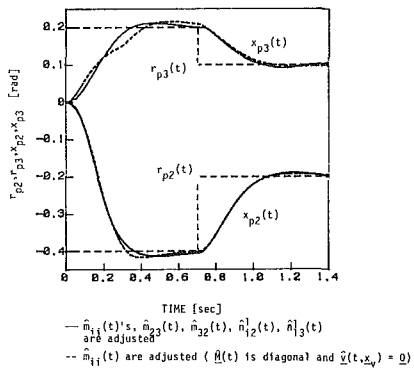

Fig. 14 Simplification of manipulator control system
(payload = 20 Kg)

responses even when the coupling terms were appreciable. The solid line in Fig. 14 represents the response of the manipulator with the adaptive controller using the gains given by (19), and the dotted line represents the response when only the diagonal elements of $\hat{\mathbf{M}}(t)$ are adjusted. It should be noted that the adaptive controller in the latter case may be compared to the adaptive scheme in [11] from the design assumption viewpoint and that the present scheme requires only one integrator for adjustment of each $\hat{m}_{ii}(t)$.

V Conclusions

A simple adaptive control scheme for mechanical manipulators was developed making use of the fundamental properties of the manipulator equations. The adaptive scheme is for compensating a nonlinear term in the dynamic equations and for decoupling the dynamic interaction. Although the scheme was presented for three degree of freedom manipulators, it can be extended to a general class of manipulators as discussed in Section II. A computer simulation study was conducted to evaluate the performance of a manipulator control system composed of the manipulator, adaptive nonlinear compensator/decoupling controller and state feedback controller with an integral action. Simulation results showed that the manipulator control system with the developed adaptive scheme is insensitive to variations of manipulator configuration and payload. The simulation study also indicated that the gravitational force neglected in the MRAS controller design does not affect the response appreciably. Finally, the simulation study suggests that the present adaptive scheme can be drastically simplified by adjusting only the diagonal elements of $\hat{\mathbf{M}}(t)$.

References

1 Vudobratovic, M., Stokic, D., and Hristic, D., "New Control Concept of Antropomorphic Manipulators," *Mechanism and Machine Theory*, Vol. 12, 1978, pp. 515-530.

2 Vukobratovic, M., "Dynamics of Active Articulated Mechanisms and Synthesis of Artificial Motion," *Mechanism and Machine Theory*, Vol. 13, 1978, pp. 1-18.

3 Paul, R., "Modelling, Trajectory Calculation and Servoing of a Computer Controlled Arm," Ph.D. thesis, Stanford University, Aug. 1972.

4 Albus, J. S., "A New Approach to Manipulator Control: The Model Articulation Controller (CMAC)," ASME JOURNAL OF DYNAMIC SYSTEMS, MEASUREMENT AND CONTROL, Vol. 97, No. 3, Sept. 1975, pp. 220-227.

5 Ralbert, H. H., "Analytical Equations VS Table Look-Up for Manipulation: A Unifying Concept," *Proceedings of the 1977 IEEE Conference on Decision & Control*, 77CH1269-OCS, pp. 576-579.

6 Yuan, J. S. C., "Dynamic Decoupling of a Remote Manipulator System," *IEEE Transactions on Automatic Control*, Vol. AC-23, No. 4, Aug. 1978.

7 Kahn, M. E., "The Near Minimum Time Control of Open Loop Articulated Kinematic Chains," Ph.D. thesis, Stanford University, 1970.

8 Hemani, H., and Camana, P. C., "Nonlinear Feedback in Simple Locomotion Systems," *IEEE Transactions on Automatic Control*, Vol. AC-21, No. 6, Dec. 1976, pp. 855-860.

Downloaded From: http://dynamicsystems.asmedigitalcollection.asme.org/ on 04/09/2015 Terms of Use: http://asme.org/terms

9 Utkin, V., "Variable Structure Systems with Sliding Modes," *IEEE Transactions on Automatic Control*, Vol. AC-22, No. 2, Apr. 1977.
10 Young, K. D., "Controller Design for a Manipulator Using Theory of Variable Structure Systems," *IEEE Transactions on Systems, Man, and Cybernetics*, Vol. SMC-8, No. 2, Feb. 1978.
11 Dubowsky, S., and DesForges, D. T., "The Application of Model Reference Adaptive Control to Robotic Manipulators," ASME JOURNAL OF DYNAMIC SYSTEMS, MEASUREMENT AND CONTROL, Vol. 101, No. 3, Sept. 1979, pp. 193–200.
12 Pieper, D. L., "The Kinematics of Manipulators Under Computer Control," Ph.D. thesis, Stanford University, 1968.
13 Paul, R., "Manipulator Cartesian Path Control," *IEEE Transactions on Systems, Man, and Cybernetics*, Vol. SMC-9, No. 11, Nov. 1979.
14 Horowitz, R., "Model Reference Adaptive Control of Mechanical Manipulators," Ph.D. thesis, University of California, Berkeley, 1983.
15 Vukobratovic, M., and Potkonjak, V., "Contribution of the Forming of Computer Methods for Automatic Modelling of Spatial Mechanisms Motions," *Mechanism and Machine Theory*, Vol. 14, 1979, pp. 179–188.
16 Pars, L. A., *A Treatise on Analytical Dynamics*, Ox Bow Press, Woodbridge, Conn., 1979.
17 Potkonjak, V., and Vukobratovic, M., "Two New Methods for Computer Forming of Dynamic Equations of Active Mechanisms," *Mechanism and Machine Theory*, Vol. 14, 1979, pp. 180–200.
18 Landau, Y. D., *Adaptive Control: The Model Reference Approach*, Marcel Dekker, New York, 1979.

APPENDIX I

$\mathbf{M}(\xi)$ and $\mathbf{N}^k(\xi, \dot{\xi})$ Matrices in Equations (2) and (3)

Detailed derivation of equation (2) is found in [14]. This appendix summarizes the results.

For a $2n$ degree of freedom mechanical manipulator composed of $n+1$ links connected by n cylindrical joints,

$$\begin{bmatrix} \mathbf{M}^{\theta} & \mathbf{M}^{\theta s} \\ [\mathbf{M}^{\theta s}]^T & \mathbf{M}^{s} \end{bmatrix} \begin{bmatrix} \ddot{\xi}_{\theta} \\ \ddot{\xi}_{s} \end{bmatrix} + \begin{bmatrix} \mathbf{v}_{\theta} \\ \mathbf{v}_{s} \end{bmatrix} = \begin{bmatrix} \mathbf{q}_{\theta} \\ \mathbf{q}_{s} \end{bmatrix} \tag{A1-1}$$

where

$$\mathbf{v}_{\theta} = \begin{bmatrix} v_{\theta 1} \\ \cdot \\ \cdot \\ \cdot \\ v_{\theta n} \end{bmatrix}, \quad v_{\theta k} = [\dot{\xi}_{\theta}^T \dot{\xi}_{s}^T] \begin{bmatrix} \mathbf{N}_{\theta}^{k\theta} & \mathbf{N}_{\theta}^{ks} \\ [\mathbf{N}_{\theta}^{ks}]^T & \mathbf{0} \end{bmatrix} \begin{bmatrix} \dot{\xi}_{\theta} \\ \dot{\xi}_{s} \end{bmatrix} \tag{A1-2}$$

and

$$\mathbf{v}_{s} = \begin{bmatrix} v_{s1} \\ \cdot \\ \cdot \\ \cdot \\ v_{sn} \end{bmatrix}, \quad v_{sk} = [\dot{\xi}_{\theta}^T \dot{\xi}_{s}^T] \begin{bmatrix} \mathbf{N}_{s}^{k} & \mathbf{N}_{s}^{ks} \\ [\mathbf{N}_{s}^{ks}]^T & \mathbf{0} \end{bmatrix} \begin{bmatrix} \dot{\xi}_{\theta} \\ \dot{\xi}_{s} \end{bmatrix} \tag{A1-3}$$

Matrices in equations (A1-1)–(A1-3) are defined as follows:

$$m_{ij}^{\theta} = m_{ji}^{\theta} = \sum_{k=\max(i,j)}^{n} \{ m_k [\mathbf{u}_i \times (\mathbf{g}_k - \mathbf{r}_i)]^T [\mathbf{u}_j \times (\mathbf{g}_k - \mathbf{r}_j)] + \mathbf{u}_i^T \mathbf{I}_k \mathbf{u}_j \} \tag{A1-4}$$

where m_k is the mass of link k, $\mathbf{I}_k$ is the moment of inertia matrix of link k about the mass center, and all other variables are as defined in Section II.

$$m_{ij}^{\theta s} = \sum_{k=\max(i,j)}^{n} m_k \mathbf{u}_i^T [\mathbf{u}_j \times (\mathbf{g}_k - \mathbf{r}_j)] \tag{A1-5}$$

$$m_{ij}^{s} = m_{ji}^{s} = \sum_{k=\max(i,j)}^{n} m_k \mathbf{u}_i^T \mathbf{u}_j \tag{A1-6}$$

$$n_{\theta ij}^{k\theta} = n_{\theta ji}^{k\theta} = \sum_{l=\max(k,j)}^{n} \{ m_l [\mathbf{u}_k \times (\mathbf{g}_l - \mathbf{r}_k)]^T [\mathbf{u}_i \times (\mathbf{u}_j \times (\mathbf{g}_l - \mathbf{r}_j))] + \mathbf{u}_k^T \left[\frac{1}{2} \mathrm{trace}(\mathbf{I}_l) \mathbf{u}_i \times \mathbf{u}_j + \mathbf{u}_j \times \mathbf{I}_l \mathbf{u}_i \right] \}, \quad i \le j \tag{A1-7}$$

where

$$\mathrm{trace}(\mathbf{I}_l) = I_{l11} + I_{l22} + I_{l33}$$

$$n_{\theta ij}^{ks} = \begin{bmatrix} \sum_{l=\max(k,j)}^{n} m_l [\mathbf{u}_k \times (\mathbf{g}_l - \mathbf{r}_k)]^T [\mathbf{u}_i \times \mathbf{u}_j] & , \ i \le j \\ 0 & , \ i > j \end{bmatrix} \tag{A1-8}$$

$$n_{sij}^{k\theta} = n_{sji}^{k\theta} = \sum_{l=\max(k,j)}^{n} m_l \mathbf{u}_k^T [\mathbf{u}_i \times (\mathbf{u}_j \times (\mathbf{g}_l - \mathbf{r}_k))], \quad i \le j \tag{A1-9}$$

$$n_{sij}^{ks} = \begin{bmatrix} \sum_{l=\max(k,j)}^{n} m_l \mathbf{u}_k^T [\mathbf{u}_i \times \mathbf{u}_j] & , \ i \le j \\ 0 & , \ i > j \end{bmatrix} \tag{A1-10}$$

APPENDIX II

Proof of Lemma in Section II

Since Property B and the symmetry of $\mathbf{M}$ are obvious from inspection of equations (A1-4)–(A1-10), a proof is given only for $\mathbf{M} > 0$ assuming that all joints are cylindrical.

Writing the positive nonsingular moment of inertia matrix of link k as

$$\mathbf{I}_k = \mathbf{S}_k \mathbf{S}_k \ (\mathbf{S}_k = \text{nonsingular } 3 \times 3 \text{ matrix}) \tag{A2-1}$$

the product $\mathbf{u}_i^T \mathbf{I}_k \mathbf{u}_j$ can be expressed as

$$\mathbf{u}_i^T I_k \mathbf{u}_j = [\mathbf{S}_k \mathbf{u}_i]^T [\mathbf{S}_k \mathbf{u}_j] \tag{A2-2}$$

Define two sets of 3 dimensional vectors, j_{ik}'s and l_{ik}'s by

$$\left. \begin{aligned} \mathbf{j}_{ik} &= \mathbf{S}_k \mathbf{u}_i \\ \mathbf{l}_{ik} &= \mathbf{u}_i \times (\mathbf{g}_k - \mathbf{r}_i) \end{aligned} \right\} \tag{A2-3}$$

and two sets of 3 $2n$ matrices, $\mathbf{Q}_k$'s and $\mathbf{R}_k$'s by

$$\left. \begin{aligned} \mathbf{Q}_k &= \sqrt{m_k} [\mathbf{I}_{1k} \ldots \mathbf{I}_{kk} \mathbf{0} \ldots \mathbf{0} \mathbf{u}_1 \ldots \mathbf{u}_k \mathbf{0} \ldots \mathbf{0}] \\ \mathbf{R}_k &= [\mathbf{j}_{1k} \ldots \mathbf{j}_{kk} \mathbf{0} \ldots \mathbf{0} \mathbf{0} \ldots \mathbf{0}] \end{aligned} \right\} \tag{A2-4}$$

Then noting equations (A1-4)–(A1-6) and (A2-2), the generalized inertia matrix $\mathbf{M}$ can be written as

$$\mathbf{M} = \sum_{k=1}^{n} (\mathbf{Q}_k^T \mathbf{Q}_k + \mathbf{J}_k^T \mathbf{J}_k) \tag{A2-5}$$

Noting $\mathbf{u}_k \neq \mathbf{0}$, $\mathbf{j}_{kk} = \mathbf{S}_k \mathbf{u}_k \neq \mathbf{0}$ and the structure of $\mathbf{Q}_k$ and $\mathbf{R}_k$, $\mathbf{M}$ given by equation (A2-5) must be positive definite.

If joint i is revolute (or prismatic), the $(n+i)$th (or ith) column drops from $\mathbf{Q}_k$ and $\mathbf{R}_k$ and their dimensions become $3 \times (2n-1)$. $\mathbf{M}$ matrix given by equation (A2-5) becomes $(2n-1) \times (2n-1)$, and is still nonsingular because of the same reason as before. Repeating this argument, $\mathbf{M} > 0$ can be shown for any combinations of cylindrical, revolute, and prismatic joints.

APPENDIX III

Stability Proof of the MRAS Nonlinear Compensator/ Decoupling Controller

The stability of the MRAS defined by equations (11)–(14) is proved by the Popov hyperstability [18] assuming the $\mathbf{M}$ and $\mathbf{N}_k$'s remain constant during the adaptation.

Subtracting equation (6) from equation (10), and using equations (11) and (12),

Downloaded From: http://dynamicsystems.asmedigitalcollection.asme.org/ on 04/09/2015 Terms of Use: http://asme.org/terms

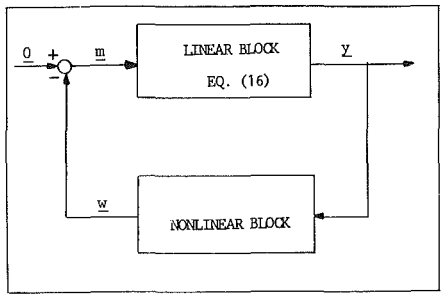

Fig. A1 Popov loop for MRAS nonlinear compensator/decoupling controller

$$\mathbf{M}\ddot{\mathbf{e}}(t)+\mathbf{F}_v\dot{\mathbf{e}}(t)+\mathbf{F}_p\mathbf{e}(t)=\mathbf{m}(t) \tag{A3-0}$$

where $\mathbf{e}(t)$ is the error between the reference model and the manipulator angular rotation vector, as defined by equation (15) and

$$\mathbf{m}(t)=(\mathbf{M}-\hat{\mathbf{M}}(t))\mathbf{u}(t)+(\mathbf{v}(\mathbf{x}_v(t))-\hat{\mathbf{v}}(\mathbf{x}_v(t))) \tag{A3-1}$$

$$\mathbf{v}(\mathbf{x}_v(t))-\hat{\mathbf{v}}(\mathbf{x}_v(t))=\begin{bmatrix}\mathbf{x}_v{}^T(\mathbf{N}^1-\hat{\mathbf{N}}^1(t))\mathbf{x}_v\\ \mathbf{x}_v{}^T(N^2-\hat{\mathbf{N}}^2(t))\mathbf{x}_v\\ \mathbf{x}_v{}^T(\mathbf{N}^3-\hat{\mathbf{N}}^3(t))\mathbf{x}_v\end{bmatrix} \tag{A3-2}$$

Defining $\mathbf{x}^T(t)=[\mathbf{e}^T(t)\dot{\mathbf{e}}^T(t)]^T$, equation (A3-0) can be written in matrix form:

$$\frac{d}{dt}\mathbf{x}(t)=\begin{bmatrix}\mathbf{0} & \mathbf{I}\\ -\mathbf{M}^{-1}\mathbf{F}_p & -\mathbf{M}^{-1}\mathbf{F}_v\end{bmatrix}\mathbf{x}(t)+\begin{bmatrix}\mathbf{0}\\ \mathbf{M}^{-1}\end{bmatrix}\mathbf{m}(t) \tag{A3-3}$$

From equation (14)

$$\mathbf{y}(t)=[\mathbf{C}_p\mathbf{C}_v]\mathbf{x}(t) \tag{A3-4}$$

The transfer matrix from $\mathbf{m}$ to $\mathbf{y}$ is given by equation (16).

By considering that $\mathbf{m}(t)$ is a function of $\mathbf{y}(t)$, we can represent equations (A3-1)–(A3-4) and the adaptation algorithm (13) by the Popov loop shown in Fig. A1.

The linear feedforward block, given by the transfer matrix $\mathbf{G}(s)$, is strictly positive real when the matrices $\mathbf{C}_p$, $\mathbf{C}_v$, $\mathbf{F}_p$, and $\mathbf{F}_v$ are selected such that equations (17) and (18) are satisfied [14].

In order to show that the equivalent feedback structure (Popov Loop) in Fig. A1 is an asymptotically hyperstable system, it is necessary to show the following propositions.

Proposition A3.1. The feedback nonlinear block in Fig. A.1 with input $\mathbf{y}$ and output $\mathbf{w} = -\mathbf{m}$ satisfies the Popov inequality,

$$\int_0^t \mathbf{w}^T(\tau)\mathbf{y}(\tau)\mathbf{d}\tau \geq -\gamma_0{}^2 \text{ for all } t\geq 0 \tag{A3-5}$$

where γ_0 is a constant which is function of the initial conditions.

Proposition A3.2. $\mathbf{u}(t)$, $\mathbf{x}_p(t)$, $x_v(t)$, $\hat{\mathbf{x}}_p(t)$ and $\hat{\mathbf{x}}_v(t)$ are bounded vector functions.

Proof of A3.1. From equations (A3-1) and (A3-2), the inner product of the input and output of the nonlinear feedback block is

$$\mathbf{w}^T(t)\mathbf{y}(t)=\sum_{i=1}^{3}\sum_{j=1}^{3}[\hat{m}_{ij}(t)-m_{ij}]f_{mij}(t) \tag{A3-6}$$

$$+\sum_{k=1}^{3}\sum_{i=1}^{3}\sum_{j=1}^{3}[\hat{n}^k{}_{ij}(t)-n^k{}_{ij}]f^k{}_{nij}(t)$$

where

$$f_{mij}(t)=y_i(t)u_j(t);\quad i=1,2,3, j=1,2,3 \tag{A3-7}$$

$$f^k{}_{nij}(t)=y_k(t)x_{vi}(t)x_{vj}(t);\quad k=1,2,3,\ i=1,2,3, j=1,2,3$$

From equation (7),

$$n^1{}_{11}=n^2{}_{12}=n^2{}_{13}=n^2{}_{21}=n^2{}_{22}=n^2{}_{31}=n^3{}_{12}=n^3{}_{13}=0 \tag{A3-8}$$

$$n^3{}_{21}=n^3{}_{23}=n^3{}_{31}=n^3{}_{32}=n^3{}_{33}=0$$

$$\hat{n}^1{}_{11}=\hat{n}^2{}_{12}=\hat{n}^2{}_{13}=\hat{n}^2{}_{21}=\hat{n}^2{}_{22}=\hat{n}^2{}_{31}=\hat{n}^3{}_{12}=\hat{n}^3{}_{13}=0$$

$$\hat{n}^3{}_{21}=\hat{n}^3{}_{23}=\hat{n}^3{}_{31}=\hat{n}^3{}_{32}=\hat{n}^3{}_{33}=0$$

From equations (13) and (A3-8),

$$\hat{m}_{ij}(t)=\hat{m}_{ij}(0)+k_{mij}\int_0^t f_{mij}(\tau)d\tau;\ i=1,2,3,\ j=1,2,3 \tag{A3-9}$$

$$\hat{n}^k{}_{ij}(t)=\hat{n}^k{}_{ij}(0)+k^k{}_{nij}\int_0^t f^k{}_{nij}(\tau)d\tau;\ k=1,2,3,\ i=1,2,3,$$

$$j=1,2,3$$

For $\hat{n}^k{}_{ij}$'s not included in equation (A3-7)

Integrating the first term in the right-hand side of equation (A3-6) and using (A3-9),

$$\int_0^t[\hat{m}_{ij}(\tau)-m_{ij}]f_{mij}(\tau)d\tau \tag{A3-10}$$

$$=\int_0^t\left\{\hat{m}_{ij}(0)-m_{ij}+k_{mij}\int_0^\tau f_{mij}(\eta)d\eta\right\}f_{mij}(\tau)d\tau$$

$$\geq -(\hat{m}_{ij}(0)-m_{ij})^2/2k_{mij}$$

and a similar inequality is obtained for the integral of the other term in the right-hand side of equation (A3-6). The inequality (A3-5) is concluded from (A3-10).

If equation (13′) is used instead of equation (13) (i.e., a reduced number of adjustable parameters is used) the proof of inequality (A3-5) is essentially the same as shown in equations (A3-6)–(A3-10). For details refer to [14].

Proof of A3.2. By proposition A3.1 and the fact that $\mathbf{G}(s)$ is the feedforward block of Fig. A.1, given by equation (16) is strictly positive real, using the hyperstability theorem [18] we can conclude

$$\|\mathbf{x}(t)\|\leq\delta_0(\|\mathbf{x}(0)\|+\epsilon_0),\delta_0>0,\epsilon_0>0 \tag{A3-11}$$

since

$$\mathbf{x}^T(0)=[\mathbf{e}^T(0)\dot{\mathbf{e}}^T(0)]^T=[\mathbf{0}\ \mathbf{0}]^T$$

$\mathbf{e}(t)$ and $\dot{\mathbf{e}}(t)$ are uniformly bounded.

In order to show the boundness of $\mathbf{u}(t)$, $\mathbf{x}_p(t)$ and $\mathbf{x}_v(t)$, the control law used in defining $\mathbf{u}(t)$ must be considered.

Assuming a state vector feedback controller with an integral action, $\mathbf{u}(t)$ is given by

$$\mathbf{u}(t)=\mathbf{u}_i(t)-\mathbf{K}_p\mathbf{x}_p(t)-\mathbf{K}_v\mathbf{x}_v(t) \tag{A3-12}$$

$$\frac{d}{dt}\mathbf{u}_i(t)=\mathbf{K}_i[\mathbf{r}_p(t)-\mathbf{x}_p(t)]$$

where $\mathbf{r}_p(t)$ is the reference angular position vector, and $\mathbf{K}_i$, $\mathbf{K}_p$, and $\mathbf{K}_v$ are feedback matrix gains, defined such that the matrix polynomials

$$s^3\mathbf{I}+s^2\mathbf{K}_v+s\mathbf{K}_p+\mathbf{K}_i,$$

$$s^2\mathbf{I}+s\mathbf{K}_v+\mathbf{K}_p$$

are asymptotically stable.

Downloaded From: http://dynamicsystems.asmedigitalcollection.asme.org/ on 04/09/2015 Terms of Use: http://asme.org/terms

Combining (A3-12), (15), and (10)

$$\hat{\mathbf{x}}_p(t) = [s^3\mathbf{I} + s^2\mathbf{K}_v + s\mathbf{K}_p + \mathbf{K}_i]^{-1}\{\mathbf{K}_i\mathbf{r}_p(t) - [\mathbf{K}_i + s\mathbf{K}_p + s^2\mathbf{K}_v]\mathbf{e}(t)\} \quad \text{(A3-13)}$$

where s represents the differential operator.

Since $s^3\mathbf{I} + s^2\mathbf{K}_v + s\mathbf{K}_p + \mathbf{K}_i$ is a stable matrix polynomial, and $\mathbf{r}_p(t)$ and $\mathbf{e}(t)$ are bounded vectors; by equations (A3-12) and (15) the boundness of $\mathbf{x}_p(t)$ and $\hat{\mathbf{x}}_p(t)$ can be concluded.

Similarly,

$$\hat{\mathbf{x}}_v(t) = [s^2\mathbf{I} + s\mathbf{K}_v + \mathbf{K}_p]^{-1}\{\mathbf{K}_i(\mathbf{r}_p(t) - \mathbf{x}_p(t)) + [K_p + s\mathbf{K}_v]\dot{\mathbf{e}}(t)\} \quad \text{(A3-14)}$$

From the fact that $s^2\mathbf{I} + s\mathbf{K}_v + \mathbf{K}_p$ is a stable matrix polynomial and $\mathbf{r}_p(t)$, $\mathbf{x}_p(t)$, and $\dot{\mathbf{e}}(t)$ are bounded, we can conclude that $\mathbf{x}_v(t)$ and $\hat{\mathbf{x}}_v(t)$ are bounded.

By equation (A3-12), since $\mathbf{x}_p(t)$, $\mathbf{x}_v(t)$ and $\mathbf{r}_p(t)$ are bounded and since $\mathbf{K}_i$, $\mathbf{K}_p$, and $\mathbf{K}_v$ are bounded coefficients, assuming that $\mathbf{u}(0)$ is bounded, $\mathbf{u}(t)$ can only grow exponentially. By equation (10)

$$\hat{\mathbf{x}}_v(t) = \int_0^t \mathbf{u}(\tau)d\tau + \hat{\mathbf{x}}_v(0)$$

If $\mathbf{u}(t)$ grows unbounded exponentially, so would $\hat{\mathbf{x}}_v(t)$, this contradicts the fact that $\hat{\mathbf{x}}_v(t)$ is bounded. Thus, $\mathbf{u}(t)$ is also bounded.

Downloaded From: http://dynamicsystems.asmedigitalcollection.asme.org/ on 04/09/2015 Terms of Use: http://asme.org/terms